Eur Biophys J (1988) 16:231–241

European Biophysics Journal

Molecular flexibility of extended and compacted polynucleosomes**

A steady-state fluorescence polarization study

T. Härd[1,*], P. E. Nielsen[2], and B. Norden[1,*]**

[1] Department of Physical Chemistry, Chalmers University of Technology, S-412 96 Göteborg, Sweden
[2] Department of Biochemistry, The Panum Institute, University of Copenhagen, DK-2200 Copenhagen, Denmark

Received July 29, 1987/Accepted in revised form June 9, 1988

Abstract. We have studied the effects of Na^+ (5–120 m*M*) and Mg^{2+} (0–6 m*M*) on the internal and overall flexibility of polynucleosome fragments from nuclease-solubilized chromatin from Ehrlich ascites cells. The mobility was monitored by the steady-state fluorescence polarization of the intercalated ethidium cation. The internal polynucleosome flexibility decreases continuously as the extended chromatin fragments are being compacted at increasing salt concentrations, and it can be further suppressed at ionic strengths above those where the 30 nm fiber is formed. The effect may be visualized as an initial formation of a loose 30 nm fiber that is further compacted at increasing ionic strengths. We observe several differences in the effects of Na^+ and Mg^{2+} upon chromatin compaction. First, chromatin compacted by Mg^{2+} is less flexible than that compacted by Na^+, suggesting a "tighter" chromatin structure with Mg^{2+}. Second, Mg^{2+} affects the internal mobility in polynucleosome fragments shorter than 6–7 nucleosomes, which are too short to be compacted with Na^+. Third, Mg^{2+} causes extensive macroscopic aggregation at concentrations above 0.2–0.3 m*M*, but the aggregation is uncorrelated with the intramolecular compaction. A quantitative evaluation of the overall polynucleosome "tumbling" mobility indicates that the compacted fragments possess more internal flexibility than do corresponding high molecular weight chromatin fibers. Finally, we note a correlation between the ethidium binding constant and the internal chromatin flexibility, possibly arising from lower torsional and "unwinding" flexibility of the linker DNA segments of compacted chromatin fibers.

Key words: Chromatin, polynucleosomes, chromatin condensation, DNA, flexibility, molecular mobility, ethidium, fluorescence polarization, divalent ions

Introduction

The proper folding of DNA into chromatin fibers and further into chromosomes is essential for the function of the genetic material in eukaryotic cells. While the folding of the DNA around histone octamers into nucleosomes is known in considerable detail (Richmond et al. 1984), the condensation of polynucleosomes into 30 nm fibers and further into chromosomes is still incompletely understood. There is a general consensus about the dimensions of the 30 nm fiber and the existence of a 5–6 nucleosome repeat unit (Butler 1983; Felsenfeld and McGhee 1986 (reviews)), but the orientation of the nucleosomes and the linker DNA within this fiber is very much in dispute owing to non-compatible results obtained by physical techniques such as electron microscopy (e.g. Thoma et al. 1979; Woodcock et al. 1984; Subirana et al. 1983; Greulich et al. 1987), neutron (Suau et al. 1979) and X-ray scattering (Widom and Klug 1985; Williams et al. 1986; Bordas et al. 1986; Koch et al. 1987), hydrodynamic measurements (Butler and Thomas 1980; Fulmer and Blomfield 1982) and various optical methods: electric dichroism (e.g. McGhee et al. 1983; Marquet et al. 1986), flow linear dichroism (Tjerneld et al. 1982; Makarov et al. 1983, 1985, 1987; Kubista et al. 1985, 1988), electric birefringence (Marion 1984; Harrington 1985) and light scattering (Marion et al. 1981). Thus several models for the 30 nm fiber have been presented in the literature (Felsenfeld and McGhee 1986 (review); Subirana et al. 1983; Makarov et al. 1985; Nielsen 1985; Williams et al. 1986; Bordas et al. 1986; Kubista et al. 1988).

Chromatin condensation is induced by cations such as Na^+ on Mg^{2+} but also by spermine, spermidine, Mn^{2+}, Cu^{2+}, Co^{2+} (Sen and Crothers 1986),

* Present address: Department of Medical Biophysics, Karolinska Institute, S-10401 Stockholm, Sweden
** This project is supported by the Swedish Natural Research Council. P.E.N. is the recipient of a Hallas-Møller Fellowship through the NOVO Foundataion
*** To whom offprint requests should be sent
Abbreviations: FPA, fluorescence polarization anisotropy; CT, calf thymus; HMW, high molecular weight; ARF, amplitude reduction factor; kbp, kilobasepairs

and recent studies have indicated that the structure of the condensed chromatin is not independent of the condensing ion (Widom 1986).

Here we present a study of the overall and internal mobility of extended and compacted polynucleosomes as it is reflected in the steady-state fluorescence polarization anisotropy (FPA) of the intercalated ethidium cation. Intercalating dyes have been shown to bind primarily to linker DNA regions (Angerer and Moudrianakis 1972; Paoletti et al. 1977; Genest et al. 1981; Kubista et al. 1985). The FPA therefore reflects the torsional mobility of the linker DNA (Ashikawa et al. 1983, 1985) as well as "segmental" mobility of nucleosomes within the fiber, and also overall tumbling mobility of the polynucleosomes. The contributions of different motions can be extracted by comparing the FPA of polynucleosomes and high molecular weight (HMW) chromatin studied under the same experimental conditions.

We have been particularly interested in differences between polynucleosomes that are exposed to Na^+ or Mg^{2+} as condensing agents.

The effects of Mg^{2+} have been studied by physical methods. Thoma et al. (1979) prepared electron micrographs, on which the degree of compaction can be compared at different NaCl and $MgCl_2$ concentration and recent studies have shown that chromatin condensation by Mg^{2+} produces larger aggregates of 30 nm fibers which is not observed with Na^+ (Widom 1986). Ashikawa et al. (1983, 1985) used the time-resolved FPA decay of ethidium to measure the internal flexibility in high molecular weight chromatin for various ionic conditions. McGhee et al. (1980 and 1983) used electric dichroism to study the DNA arrangement within the Mg^{2+}-compacted fiber. Sen and Crothers (1986) subsequently compared the effects of several multivalent cations upon chromatin compaction. The $MgCl_2$ induced compaction has also been studied using circular dichroism (Watanabe and Koujiro 1984).

We observe several differences in the effects of Na^+ and Mg^{2+} on the internal and overall mobility, which we attribute to a "tighter" packing with Mg^{2+}. In particular, we note that Mg^{2+} affects the mobility of polynucleosomes that are too short to be condensed by Na^+. Furthermore, there is a continuous decrease in the internal flexibility when excess salt is added after formation of the 30 nm fiber. This decrease is not correlated with the simultaneously occurring intermolecular aggregation (Sen and Crothers 1986). Finally, we discuss an observed decrease in the stability of the DNA/ethidium complex upon chromatin compaction.

Materials and methods

Materials. Ehrlich ascites cells were grown intraperitonally in mice, and nuclei from these cells were prepared using a modification of a published (Lerner and Steitz 1979) procedure: 9 grams (wet weight) of cells were washed (2,000 *g*/5 min) in 150 ml 150 m*M* NaCl, 10 m*M* Tris-HCl at pH 7.4, resuspended in 150 ml 140 m*M* NaCl, 1.5 m*M* $MgCl_2$, 0.5% Nonidet P40, 10 m*M* Tris-HCl at pH 7.5 and homogenized at 0 °C with 10 strokes in a Dounce homogenizer. The nuclei were isolated by centrifugation (3,000 *g*/20 min) through a 50 ml sucrose cushion (0.8 *M* sucrose, 5 m*M* $MgCl_2$, 1% Nonidet P40, 10 m*M* tris-HCl at pH 7.5), and resuspended in 20 ml digestion buffer (0.34 *M* sucrose, 60 m*M* KCl, 15 m*M* NaCl, 1 m*M* $CaCl_2$, 0.5% Nonidet P40, 10 m*M* Tris-HCl at pH 7.4). 300 units of micrococcus nuclease (Boehringer, Mannheim, FRG) were added and the nuclei suspension was incubated at 37 °C for 15 min. The nuclei were reisolated by centrifugation (5,000 *g*/5 min) and extracted with 10 ml 1 m*M* EDTA at pH 8 and 0 °C. The 10,000 *g* (10 min) supernatant of this extract was laid on 10 ml 10–30% sucrose gradients (20 m*M* NaCl, 0.2 m*M* EDTA) (1 ml sample/gradient) and run at 39,000 rpm for 3 h in an SW40 rotor. 1 ml fractions were collected from the top of the gradient and dialyzed for 16 h at 4 °C against 0.25 m*M* EDTA, and then overnight against the experimental buffer (10 m*M* NaCl, 1 m*M* sodium cacodylate, 0.1 m*M* EDTA at pH 7). Average polynucleosome sizes were measured by running the samples along with markers from a Hind III digestion of lambda DNA on an agarose gel. The monodispersity was estimated to within ~40% (90% material) of the average polynucleosome length (Fig. 1).

Ethidium bomide (EB) was purchased from Sigma Chemical Co. and dissolved in the experimental buffer without further purification. Concentrations were determined spectrophotometrically using the extinction coefficient $\varepsilon_{260} = 13.2 \times 10^3\ M$ DNA base pairs^{-1} cm^{-1} for the chromatin and $\varepsilon_{477} = 5.6 \times 10^3$ for EB (Waring 1965). In preparing the chromatin/dye samples the chromatin was added to a dilute dye solution to avoid high local dye concentrations. The dye/DNA base pair ratio was kept low (typically 0.015) to avoid distortion of the chromatin conformation (Kubista et al. 1985). The ionic strength was adjusted during the fluorescence titrations by adding small volumes of more concentrated NaCl and $MgCl_2$ solutions. The Mg^{2+} concentrations referred to below have been corrected for the presence of EDTA in the samples.

Calf Thymus (CT) DNA was purchased from Sigma and dialyzed against the experimental buffer without further purification.

Fluorescence measurements. Fluorescence polarization was measured on an Aminco SPF-500 spectrofluorometer using Polaroid sheet polarizers in the excitation and emission paths. The steady-state fluorescence

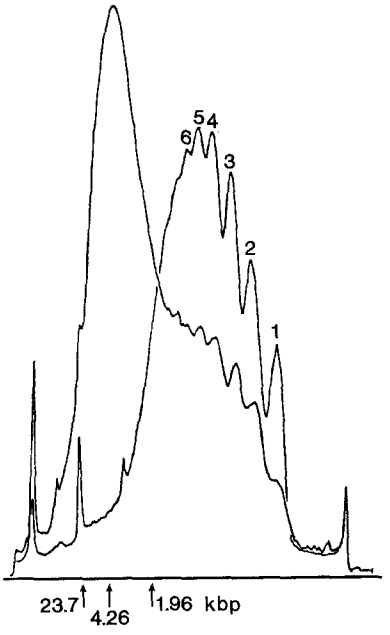

A

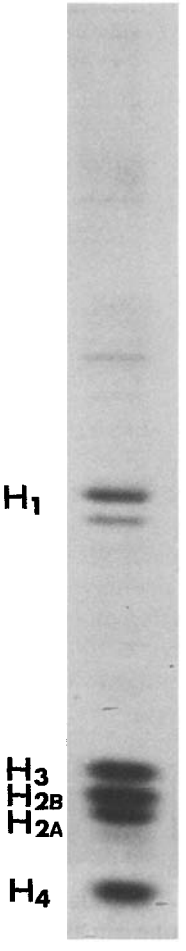

B

polarization anisotropy (r) was calculated from

$$\bar{r}=\frac{I_{VV}\times G-I_{VH}}{I_{VV}\times G+2I_{VH}} \quad (1)$$

where I denotes fluorescence intensity, the subscripts refer to vertical and horizontal positioning of the excitation and emission polarizers, respectively, and $G=I_{HH}/I_{HV}$ corrects for polarizing effects in the emission monochromator and the detector. The errors in the FPA measurements are indicated as error bars in Fig. 3 (estimated standard deviations). The total fluorescence intensity was taken to be proportional to the denominator of Eq. (1). The temperature was 20 ± 0.5 °C in all experiments.

The FPA was corrected for contributions to the depolarization from unbound dye molecules using the relation

$$I_{\text{obs}}\,\bar{r}_{\text{obs}}=f_{\text{bound}}\,I_{\text{bound}}\,\bar{r}_{\text{bound}}+(1-f_{\text{bound}})\,I_{\text{free}}\,\bar{r}_{\text{free}} \quad (2)$$

where I_{free} and $\bar{r}_{\text{free}}$ were measured separately at identical instrumental settings. The fraction of bound dye, f_{bound}, was calculated from the observed fluorescence intensity, as described in the Results section.

Static light scattering was measured on the spectrofluorometer with both the excitation and emission monochromators set on 700 nm.

Theory

Several effects contribute to the fluorescence depolarization of ethidium intercalated in polynucleosome fragments. First, the dye is not rigidly attached to the DNA, but undergoes restricted librational motions within the intercalative pocket with a correlation time of ~100 ps (Magde et al. 1983). Second, there will be a depolarization owing to the internal mobility in the linker DNA segment (Ashikawa et al. 1983). This mobility has previously been considered to be purely torsional in character (Ashikawa et al. 1983, 1985; Shibata et al. 1985), but there is recent evidence that it may also contain some contribution of "out-of-plane" mobility (Härd 1987). Third, there will be a "segmental" mobility of the nucleosomes in the HMW chromatin fiber and overall tumbling mobility of the polynucleosome fragments. Finally, intramolecular energy transfer between ethidium molecules inter-

Fig. 1. **A** Densitometer scans following gel electrophoresis of two polynucleosome samples used in this study. The peaks corresponding to the shortest oligomers and also the bands of some of the "marker" DNA restriction fragments are indicated. The average polynucleosome lengths of these two samples were estimated as 24 and 5 nucleosomes (left and right curves, respectively). **B** Histone content of a typical nucleosome preparation. Coomassie-stained SDS-polyacrylamide gel

calated in the same linker DNA segment will cause additional depolarization (Genest et al. 1981).

Assuming that all these effects are uncorrelated, a model of the time dependent FPA can be written (Szabo 1984)

$$r(t) = r_M(t) \times \mathrm{ARF}_w \times \mathrm{ARF}_{ET}\{\langle P_2\rangle^2 + (1-\langle P_2\rangle^2)\exp(-t/\tau_{\mathrm{int}})\}. \quad (3)$$

In this equation, ARF_w and ARF_{ET} are amplitude reduction factors due to rapid dye librations and intramolecular energy transfer, respectively. ARF_w has been experimentally determined (Magde et al. 1983). ARF_{ET} will depend on the dye/DNA base pair ratio, and it will approach unity (i.e. no effect) when this ratio is close to zero. In this study ARF_{ET} is obtained as the ratio of the observed steady-state FPA to the FPA extrapolated to zero dye concentration (Fig. 6). The expression between the brackets in Eq. (3) is an approximate correlation function for isotropic restricted internal mobility in the linker DNA and isotropic segmental nucleosome motions (Kinosita et al. 1977; Szabo 1984). The parameters $\langle P_2\rangle$ and τ_{int} are the first (non-trivial) order parameters due to the restricted mobility (Heyn 1979) and the effective rotational correlation time, respectively. The order parameter, $\langle P_2\rangle$, can be extracted from recently published time-resolved FPA data (Ashikawa et al. 1983, 1985).

The overall mobility of the polynucleosome fragments cannot, in general, be considered to be isotropic. In the case of cylindrical overall polynucleosome symmetry the anisotropy for the overall mobility, $r_M(t)$, is a triple exponential containing linear combinations of the rotational diffusion constants, $D_{\|}$ and $D_{\perp}$, for motions about the two principal cylinder axes. However, we cannot unambiguously distinguish between these two rates of anisotropic macromolecular rotations. Therefore, we introduce an "effective" correlation time, τ_M, to describe the overall polynucleosome mobility, yielding

$$r_M(t) = \tfrac{2}{5}\exp(-t/\tau_M). \quad (4)$$

In the expression for the steady-state FPA, to be derived below, the effective correlation time is the harmonic mean of the two correlation times for "cylindrical" overall mobility, $\tau_{\|}$ and $\tau_{\perp}$ (Cantor and Schimmel 1983), i.e.

$$\frac{1}{\tau_M} = \frac{1}{3}\left(\frac{1}{\tau_{\|}} + \frac{2}{\tau_{\perp}}\right). \quad (5)$$

Under continuous illumination of the sample, the time averaged anisotropy becomes

$$\bar{r} = \int_0^{\infty} r(t)(1/\tau_F)\exp(-t/\tau_F)\,\mathrm{d}t \quad (6)$$

where τ_F is the fluorescence lifetime. Integration of Eq. (3) gives

$$\bar{r} = \tfrac{2}{5} \times \mathrm{ARF}_w \times \mathrm{ARF}_{ET}\left\{\frac{\langle P_2\rangle^2}{1+\tau_F/\tau_M} + \frac{1-\langle P_2\rangle^2}{1+\tau_F/\tau_M+t_F/\tau_{\mathrm{int}}}\right\} \quad (7)$$

which will be used in the quantitative evaluation of the overall polynucleosome mobility.

The difference in the correlation function for internal linker DNA mobility presented here and that of Ashikawa et al. (1983, 1985) requires a comment. The square of the order parameter, $\langle P_2\rangle$, in our model is identical to the a_2 parameter of the Ashikawa model. The difference between the two models is that we use an exponential to characterize the FPA decay, whereas Ashikawa et al. use the non-exponential expression for torsional DNA motions originally derived by Barkley and Zimm (1979), and Allison and Schurr (1979). Ashikawa et al. have shown that the non-exponential expression is a better approximation of the true FPA decay of ethidium bound to the linker DNA when only torsional motions are possible. However, two reasons make us choose the other alternative (the single exponential) in our analysis: i) Recently we showed (Härd and Kearns 1986 a, b) that the two alternatives lead to very comparable results when the mobility is evaluated from steady-state FPA data, and that there might be some out-of-plane mobility in the complex (Härd 1987). ii) The non-exponential formulation leads to a very complicated steady-state FPA expression (J. M. Schurr, Personal communication) that is difficult to evaluate from experimental data.

Results

Fluorescence intensity and ethidium binding

Figures 2 A and B show the total fluorescence intensity of intercalated ethidium upon addition of Na^+ and Mg^{2+}, respectively. The effect of increased ionic strength is shown for three chromatin fractions containing fragments of different lengths; 5 and 14 nucleosomes, and HMW chromatin. In all cases there is a decrease in the fluorescence intensity as the ionic strength is increased. Time-resolved measurements (Ashikawa et al. 1983, 1985) show that the fluorescence quantum yield of bound ethidium is not much affected in the ionic strength intervals studied here. The observed decrease in intensity can therefore be attributed to increasing amounts of unbound dye at higher ionic strengths. (The relative fluorescence intensity of quantitatively bound ethidium is indicated in the figure.)

The binding constant at 10 mM NaCl is $K = 1.0 \times 10^6\, M^{-1}$ (Paoletti et al. 1977), and one can assume the binding site density to be $0.5 \times 20/160 = 0.0625$

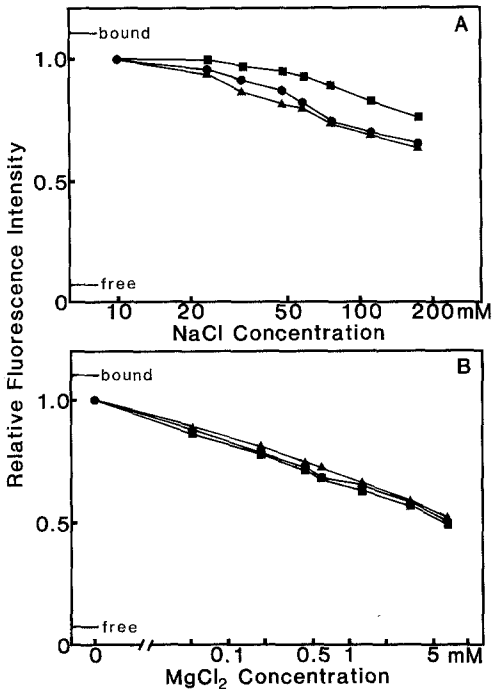

Fig. 2 A and B. Fluorescence intensity of intercalated ethidium as a function of NaCl (**A**) and $MgCl_2$ (**B**) concentration, for polynucleosomes (5 nucleosomes (■) and 17 nucleosomes (●)), HMW chromatin (▲), and CT DNA (▼). Excitation and emission wavelengths 520 and 620 nm. The concentrations are 150 μ*M* DNA base pairs and 0.013 dye molecules/base pair. The intensities of free and quantitatively bound ethidium are indicated

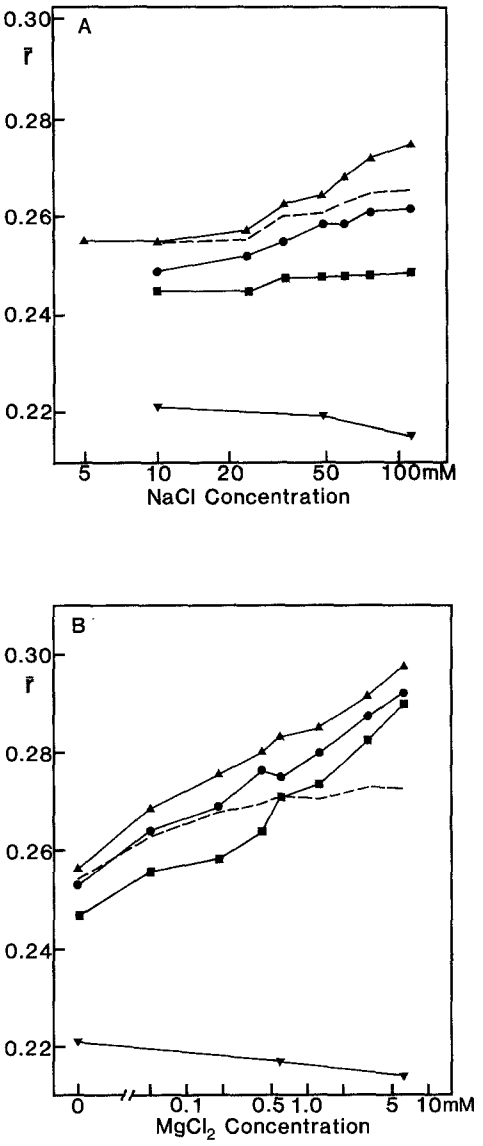

Fig. 3 A and B. Corrected FPA of intercalated ethidium as a function of NaCl (**A**) and $MgCl_2$ (**B**) concentration (m*M*), for polynucleosomes (5 nucleosomes (■) and 17 nucleosomes (●)), HMW chromatin (▲), and CT DNA (▼). (The uncorrected data for the HMW chromatin fraction are indicated with a *dashed line*.) Experimental conditions as in Fig. 1

(DNA base pairs)$^{-1}$ reflecting available binding sites in the linker DNA in Ehrlich ascites cell chromatin (Kubista et al. 1985; P. E. Nielsen, unpublished results). Using these data we calculated apparent binding constants at the higher salt concentrations from observed fluorescence intensities. At 100 m*M* NaCl the binding constant was $2.4 \times 10^5\ M^{-1}$ which compares well with the 5-fold decrease in ethidium between 10 and 100 m*M* NaCl observed by Angerer and Moudrianakis (1972) on sheared chromatin.

Note (in Fig. 2) that ethidium in the shorter fragment is less affected by NaCl addition than in the HMW chromatin, whereas $MgCl_2$ addition affects the ethidium binding equally in all chromatin fractions.

Fluorescence polarization of intercalated ethidium

The effects of Na^+ and Mg^{2+} addition on the FPA of intercalated ethidium are shown in Figs. 3 and 4. The FPA has been corrected for contributions from unbound ethidium, as described in the Methods section. (The uncorrected FPA values for the HMW fraction are also shown in Fig. 3, for comparison.) Figure 3 A shows the FPA of three chromatin samples (the same samples as in Fig. 2) as a function of NaCl concentration. The FPA of the polynucleosome fragments is lower than that of HMW chromatin indicating that overall polynucleosome mobility contributes to the depolarization. The FPA of the HMW fraction and the longer polynucleosome fragments (17 nucleosomes) increases with ionic strength, reflecting the decrease in internal chromatin mobility that is a result of the intramolecular compaction from an extended fiber to a condensed superstructure. This transition has a midpoint in the interval 10–40 m*M* NaCl, and is complete at 60 m*M* NaCl (Thoma et al. 1979; Widom 1986). Note that the mobility continues to decrease as NaCl

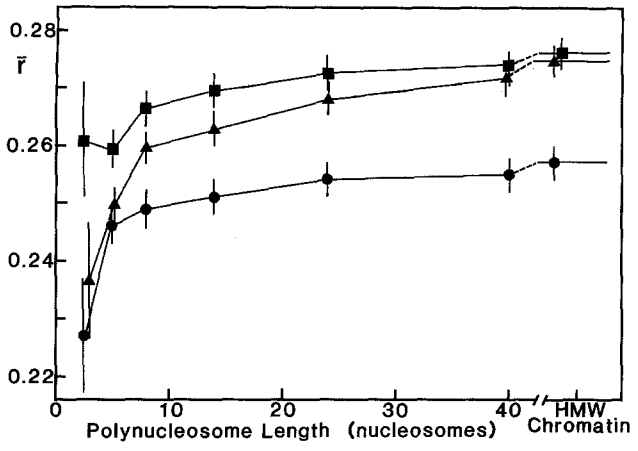

Fig. 4. Corrected FPA of intercalated ethidium as a function of polynucleosome fragment length at 10 m*M* NaCl (●), 77 m*M* NaCl (▲), and 10 m*M* $MgCl_2$ + 0.18 m*M* $MgCl_2$ (■). Experimental conditions as in Fig. 1

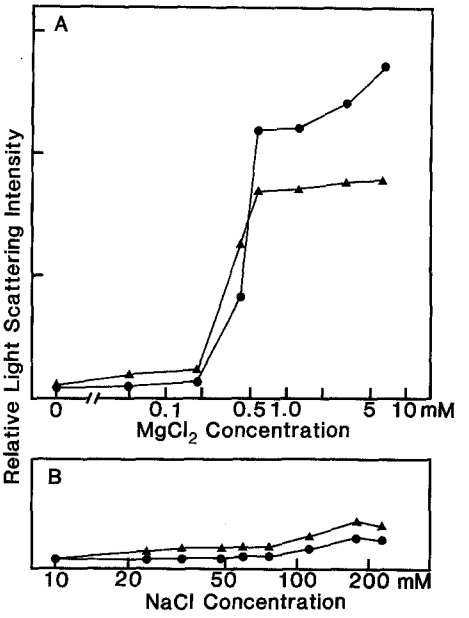

Fig. 5 A and B. The effect of $MgCl_2$ (**A**) and NaCl (**B**) concentration on the light scattering intensity (turbidity) for polynucleosomes (●) (17 nucleosomes long), and HMW chromatin (▲)

is added above this concentration. NaCl addition did not significantly affect the FPA of the short polynucleosome fragments (~5 nucleosomes long).

Figure 3 B shows the effect of $MgCl_2$ addition on the FPA of the three chromatin fractions (all samples also contained ~10 m*M* NaCl). Unexpectedly, Mg^{2+} drastically affects the FPA of all three samples. This observed decrease in molecular mobility is not caused by intermolecular aggregation, as will be shown below, although such aggregation does occur at $MgCl_2$ concentrations above 0.2 m*M* (Sen and Crothers 1986). The extended fiber to 30 nm fiber transition has been shown to be complete at 0.2–0.5 m*M* $MgCl_2$ (Thoma et al. 1979; Sen and Crothers 1986). A comparison between FPA values in this concentration range and those of the corresponding NaCl concentration interval (40–60 m*M* NaCl) shows that the FPA is significantly higher when compacted by $MgCl_2$.

Figure 4 shows the FPA of polynucleosomes in 10 and 77 m*M* NaCl, and 10 m*M* NaCl + 0.2 m*M* $MgCl_2$ as a function of fragment length. This figure clearly shows the different effects of Na^+ on pentanucleosomes versus the longer polynucleosomes. The mobility in the former sample is not much affected, whereas the fragments in the latter are obviously being compacted in 77 m*M* NaCl. Addition of Mg^{2+}, on the other hand, drastically affects the mobility in both samples.

Macroscopic aggregation at high Mg^{2+} concentrations

To monitor the extent of intermolecular chromatin aggregation we measured static light scattering under various ionic strength conditions. The effects of NaCl and $MgCl_2$ concentration on the light scattering of HMW chromatin and a polynucleosome sample are shown in Figs. 5 A and B. The scattering is low at ionic strengths below 80 m*M* NaCl and 0.2 m*M* $MgCl_2$. Above these concentrations there is a slight increase in light scattering with NaCl, whereas additional $MgCl_2$ causes a drastic increase indicating macroscopic aggregation at $MgCl_2$ concentrations above 0.2 m*M*. This critical $MgCl_2$ concentration agrees very well with that observed by Sen and Crothers (1986) in electric dichroism studies of chicken erythrocyte chromatin (0.2 to 0.25 m*M* $MgCl_2$). We did not observe any length dependence in the aggregation of different polynucleosome fragments (not shown).

Figure 6 shows the FPA and turbidity as a function of time when the $MgCl_2$ concentration is increased from 0.18 to 0.42 m*M*. It is obvious that the FPA reaches its final value within the time resolution of the measurement (a few seconds), whereas the light scattering continues to increase for more than one hour. We take this observation as an indication of uncorrelated microscopic and macroscopic condensations, i.e. the compaction within the chromatin fibers is very rapid compared to the association of fibers to each other.

Dye to dye energy transfer

Figure 7 shows the FPA as a function of the dye/DNA base pair ratio for HMW chromatin at various ionic strength conditions, and also for CT DNA. In the chromatin samples energy transfer between dyes

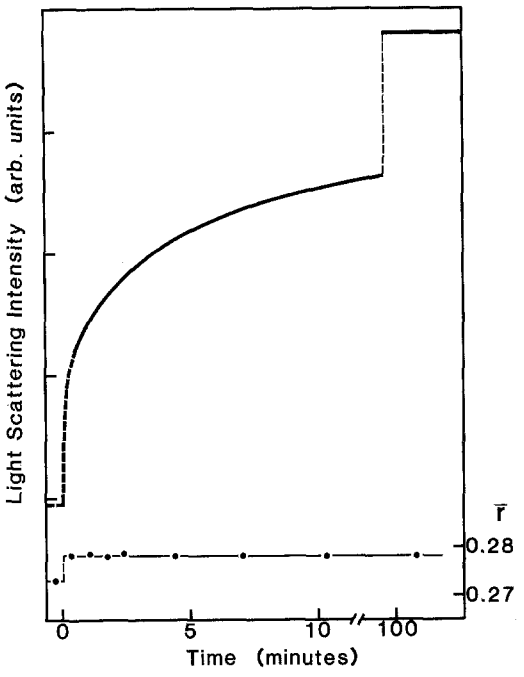

Fig. 6. Turbidity and corrected FPA of polynucleosomes (17 nucleosomes long) upon increasing the $MgCl_2$ concentration from 0.18 m*M* to 0.42 m*M*

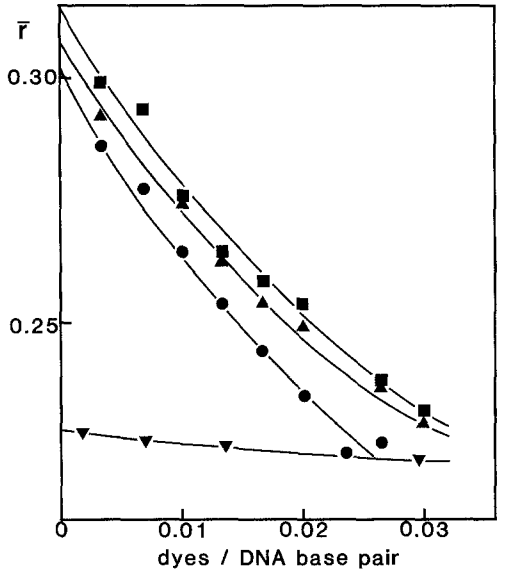

Fig. 7. Corrected FPA of intercalated ethidium as a function of the dye/DNA base pair ratio for HMW chromatin at 10 m*M* NaCl (●), 77 m*M* NaCl (▲), and 10 m*M* NaCl + 0.18 m*M* $MgCl_2$ (■), and CT DNA (▼) (10 m*M* NaCl)

located in the same linker DNA segment results in a lower FPA, as previously shown (Genest et al. 1981). Note that there are no significant differences in the extent of energy transfer between the extended fiber (in 10 m*M* NaCl) and the compacted fiber (77 m*M* NaCl or 10 m*M* NaCl + 0.18 m*M* $MgCl_2$), although the magnitude of the FPA differs between these samples. We find that the amplitude reduction factor due to energy transfer (ARF_{ET}) equals 0.85–0.87 at 0.013 dyes/DNA base pair, independent of ionic strength conditions. A shortening of the linker segment available for intercalation, upon compaction, is expected to result in a higher rate of energy transfer because the average distance between intercalated dyes would be shorter. Thus, these observations are consistent with a constant DNA linker length at the various stages of chromatin compaction.

Discussion

We have shown that the internal chromatin mobility decreases continuously when the extended fiber is compacted by NaCl or $MgCl_2$, and that the overall mobility of polynucleosome fragments is reflected in the FPA. We find that an increased NaCl concentration does not affect the mobility in fragments shorter than 6–7 nucleosomes, as expected, but that $MgCl_2$, rather unexpectedly, does affect the mobility also in the shortest polynucleosome fragments. Furthermore, polynucleosomes and HMW chromatin form macroscopic aggregates at $MgCl_2$ concentrations above 0.2 m*M*, but the aggregation is uncorrelated with the intramolecular chromatin compaction. We now discuss these effects in more detail to generate a picture of how the internal chromatin flexibility is affected by Na^+ and Mg^{2+}. In connection with this we make a quantitative evaluation of the "tumbling" mobility of the polynucleosome fragments. We also note an interesting correlation between the internal chromatin DNA mobility and the ethidium binding constant.

Continuous 10–30 nm fiber transition

We find that the FPA increases continuously upon NaCl and $MgCl_2$ addition, and we interpret this effect as a continuous decrease in the internal chromatin mobility as the extended fiber is being compacted (Finch and Klug 1976; Butler 1983; Williams et al. 1986). Electron micrographs obtained at different NaCl concentrations (Thoma et al. 1979) show that the chromatin fiber is extended in 10 m*M* NaCl and fully compacted in 60 m*M* NaCl. Therefore, one might have expected to observe a more pronounced "phase" transition in the FPA data. However, continuous behaviour upon condensation is also observed in sedimentation studies (Butler and Thomas 1980), where the sedimentation coefficient of polynucleosomes (in the size range 6.5–45 nucleosomes) show a power-law dependence between 5 and 125 m*M* NaCl, and also in light scattering studies (Marion et al. 1981; Fulmer and Bloomfield 1982).

A reasonable explanation of these continuous changes is that the flexibility within the fiber also continues to decrease after 30 nm fiber formation. One may visualize this as an initial formation of a "loose" fiber as seen on electron micrographs. The fiber is then further compacted as the ionic strength is increased, although its diameter is essentially unchanged.

Overall polynucleosome tumbling

The lower FPA of the polynucleosomes compared to the HMW chromatin is due to larger overall rotational mobility of the polynucleosome fragments, and a quantitative evaluation of this "tumbling" mobility at different ionic strength conditions can be made. The different parameters of Eq. (7) for the various conditions are listed in Table 1. The amplitude reduction factor due to dye wobbling, ARF_w, is assumed to be the same as in the non-nucleosomal DNA, i.e. $ARF_w = 0.925$ (Magde et al. 1983; Shibata et al. 1985), and the amplitude reduction factors due to energy transfer ARF_{ET} are obtained from Fig. 6, as explained in the Theory section. The fluorescence lifetimes of intercalated ethidium, τ_F, and the order parameters, $\langle P_2 \rangle$, for the restricted internal mobility are taken from the time-resolved fluorescence studies of Ashikawa et al. (1985).

The correlation times, τ_M, for overall polynucleosome mobility (tumbling times) are calculated in the following way. The correlation times for the internal chromatin mobility, τ_{int}, are calculated from the FPA of the HMW DNA with the assumption that $\tau_M \gg \tau_{int}$ (Ashikawa et al. 1985). The tumbling times of the polynucleosomes are then calculated assuming that the internal chromatin mobility is unchanged in the polynucleosome fragments. The results are shown in Table 2. Also indicated in this table are the expected fiber dimensions for Ehrlich ascites cell chromatin (linker DNA length of 20 base pairs) according to Williams et al. (1985), and the effective rotational correlation times for anisotropic rotations of the corresponding rigid bodies (oblate and prolate ellipsoids with the same volume as the solenoid) (Cantor and Schimmel 1980). The tumbling times of the extended fragments are, in general, longer than in the compacted state. This is reasonable, because an elongated body is expected to rotate more slowly than a more spherically shaped one with the same volume.

All experimental tumbling times in the compacted state are significantly shorter than expected for rigid overall tumbling. This could indicate that the calculated overall solenoid dimensions are too large. However, this is not likely, because it does not seem to be possible to pack the fragments within a volume small enough to bring calculated and rotational rates in agreement. Also, alternative models of the 30 nm fiber (e.g. Finch and Klug 1976) have similar dimensions. Therefore, the polynucleosomes must possess some internal mobility, i.e. "segmental" motions of the nucleosomes within the fragment. Note that the segmental mobility that is present also in the HMW chromatin has already been accounted for in τ_{int}, because τ_M was assumed to be very large in the HMW chromatin. Consequently, there is some "extra" internal flexibility in the polynucleosomes. The effect might be caused by an insufficient number of stabilizing internucleosome contacts in the fragments. Furthermore, there is less internal mobility when the fragments are compacted in $MgCl_2$ (0.2 m*M*) than in NaCl (77 m*M*) as judged from the longer tumbling times, although electron micrographs indicate the same "degree of compaction" in the two cases (or even more compaction in the NaCl compacted fragments) (Thoma et al. 1979). This observation is further discussed below.

Table 1. FPA parameters for HMW chromatin under various ionic conditions

	10 m*M* NaCl	77 m*M* NaCl	0.2 m*M* $MgCl_2$
τ_F [a]	23.6 ns	23.3 ns	23.3 ns
ARF_w [b]	0.925	0.925	0.925
ARF_{ET}	0.84	0.86	0.86
$\langle P_2 \rangle$ [a]	0.775 [a, c]	0.824 [a, d]	0.842 [a, e]
FPA_{HMW}	0.2564	0.2740	0.2756
τ_{int}	6.7	6.2	4.2

[a] Ashikawa et al. (1985) (values for chicken erythrocyte chromatin)
[b] Magde et al. (1983)
[c] 1 m*M* Tris, 0.2 m*M* EDTA, pH 7.5, $T = 20$ °C
[d] 1 m*M* Tris, 0.2 m*M* EDTA, 50 m*M* NaCl, pH 7.5, $T = 20$ °C
[e] 10 m*M* Tris, 10 m*M* NaCl, 0.47 m*M* $MgCl_2$, pH 7.5, $T = 20$ °C

Table 2. Correlation times for overall polynucleosome tumbling

Polynucl. Length/ nuclsms	Conditions	Rotnl. corr. time $\tau_M/\mu s$		Fiber dimensions nm	
		(exp.)	(calc.)	diameter	length
8	10 m*M* NaCl	1.0			
	77 m*M* NaCl	0.5			
	0.2 m*M* $MgCl_2$	1.0	3.1	24	17
14	10 m*M* NaCl	1.3			
	77 m*M* NaCl	0.7			
	0.2 m*M* $MgCl_2$	1.5	3.3	24	30
24	10 m*M* NaCl	3.8			
	77 m*M* NaCl	1.4			
	0.2 m*M* $MgCl_2$	2.3	5.4	24	51
40	10 m*M* NaCl	4.6			
	77 m*M* NaCl	1.8			
	0.2 m*M* $MgCl_2$	2.8	9.7	24	86

Tighter chromatin packing with Mg^{2+}

We observe several differences in the action of Mg^{2+} and Na^+ in comparing the chromatin fiber (apart from the fact that Mg^{2+} is active at much lower concentrations than is Na^+). i) $MgCl_2$ affects the mobility in polynucleosome fragments that have been shown to be too short to form a compact fiber structure with NaCl (Butler and Thomas 1980; Marion et al. 1981; Marion 1984; Chauvin et al. 1985). It is not clear whether or not these fragments are being compacted by Mg^{2+} or if the linker DNA mobility is reduced while the fragment is still the extended form. ii) The internal mobility is lower in the $MgCl_2$ compacted fibers at the critical ionic strengths for solenoid formation. Electron micrographs show that the "degree of compaction" is the same in samples containing 40 and 60 m*M* NaCl, as in samples with 0.2 and 0.5 m*M* $MgCl_2$, respectively (Thoma et al. 1979). A comparison between the FPA data in Figs. 2 A and B shows that the internal mobility in the HMW fiber is significantly lower with Mg^{2+} at these two corresponding ionic conditions. iii) The same effect is observed in the polynucleosome fragments, as judged from the calculated tumbling times in Table 2.

On the basis of these observations we suggest that Mg^{2+} forces the chromatin fiber into a "tighter" conformation, i.e. conformation with less internal flexibility, than does Na^+. Thus, the extent of internal chromatin flexibility depends on both the ionic strength and the particular counterion by which it is being condensed. This behaviour is in accordance with the continuous decrease in internal fiber mobility upon condensation, as well as the synergistic effects of different multivalent cations discussed by Sen and Crothers (1986).

Using only the present data it is difficult to give a detailed mechanism for the tighter chromatin packing with Mg^{2+}. It is likely however, that Mg^{2+} stabilizes the fiber by promoting DNA-DNA interactions between consecutive linker DNA segments. Such a mechanism might also explain why the shortest polynucleosomes seem to be compacted by Mg^{2+}: With Na^+, the limited number of internucleosome contacts are not enough to stabilize a 30 nm fiberlike conformation, whereas Mg^{2+} ions also might provide specific "bridges", binding neighbouring linker DNA segments to each other. The effect is supported by recent studies of associated/aggregated DNA fragments (Härd and Kearns 1986), where Mg^{2+}, but not Na^+, are found to stabilize the aggregates.

Several models for the structure of the 30 nm fiber have been proposed during the past decade. On the basis of the orientation of the nucleosome cores (roughly parallel versus perpendicular to the fiber axis) and the path of the linker DNA (supercoiled versus straight "cross-wise"), they may be divided into four categories. The original solenoid model by Finch and Klug (1976) later refined by McGhee et al. (1980, 1983) have supercoiled linkers and parallel nucleosomes. "Cross-wise" linker models with *perpendicular* nucleosomes have been proposed by two groups (Makarov et al. 1985; Nielsen 1985; Kubista et al. 1988) while "cross-wise" linker models having *parallel* nucleosomes were suggested by Williams et al. (1986) and Bordas et al. (1986). Finally Worcel et al. (1981) suggested the twisted ribbon model in which the cross-wise linkers do not traverse the center of the 30 nm fiber and which have nucleosomes parallel to the fiber axis.

Our results are in agreement with those of Bordas et al. (1986), Makarov et al. (1987), Gerchman and Ramakrishnan (1987) and Greulich et al. (1987), indicating that the 10–30 nm fiber condensation is a continuous process not including distinct phases. Furthermore, the compaction by Mg^{2+} suggests a model with close linker-linker interaction, stabilized by "Mg^{2+}-bridges". Thus our results support accordion models (Makarov et al. 1985; Nielsen 1985; Bordas et al. 1986; Williams et al. 1986; Kubista et al. 1988). On the basis of our flow linear dichroism results (Tjerneld et al. 1982; Matsuoka et al. 1985; Kubista et al. 1985; Nielsen et al. (in preparation)) and similar results by Makarov et al. (1983, 1985, 1987), we favour the model with the nucleosome cores almost perpendicular to the fiber axis (Nielsen 1985; Kubista et al. 1988).

Correlation between chromatin mobility and ethidium binding

The extent of ethidium binding is reflected in the fluorescence intensity, and an apparent binding constant can thereafter be calculated from intensity data as shown above. Figure 8 is a plot of the corrected FPA of the HMW chromatin versus the apparent binding constant at different NaCl and $MgCl_2$ concentrations. The plot reveals a correlation between the mobility of the intercalative complex and the binding constant. The correlation seems to be similar for Na^+ and Mg^{2+}, as judged from the "overlap" of the plotted data points. The same effect is observed with the polynucleosome fragments: Figure 1 shows that the fluorescence intensity is less affected by NaCl addition in the shortest fragments (5 nucleosomes), in which the mobility, too, is unaffected. $MgCl_2$ addition, on the other hand, affects the fluorescence intensity, and subsequently also the mobility, in all fragments.

The following argument might provide a physical explanation to the observed effect. The torsional rigidity of the linker DNA increases upon compaction of the chromatin fiber, as shown here and in the studies

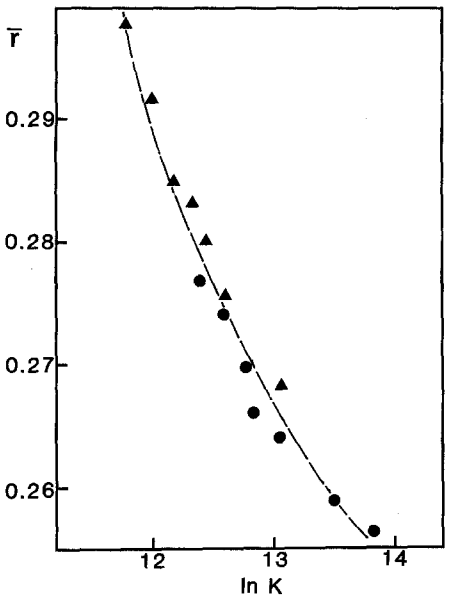

Fig. 8. Corrected FPA as a function of the apparent ethidium binding constant for HMW chromatin at various NaCl (•) and $MgCl_2$ (▲) concentrations (see text for details)

of Ashikawa et al. (1983, 1985). Therefore, more energy is needed to produce the DNA unwinding that is a prerequisite for intercalation, and the energy difference is reflected in a lower binding constant of the intercalative complex. In this way there will be a direct correlation between DNA torsional mobility and ethidium binding. However, the effect might also be a consequence of the larger shielding of the negatively charged DNA phosphates at increased salt concentrations. Since the shielding is coupled to the ionic strength it is also correlated with the decreased flexibility and the dye binding.

Conclusions

Polynucleosomes and chromatin fibers are continuously becoming less flexible at increasing ionic strength (5–120 m*M* NaCl and 0–6 m*M* $MgCl_2$), and the internal flexibility of chromatin in the compacted conformation can be further suppressed by addition of "excess" salt. Compacted polynucleosome fragments exhibit more internal flexibility than do compacted high molecular weight chromatin fibers.

Chromatin fibers and polynucleosome fragments compacted by Mg^{2+} are less flexible than those compacted by Na^+ at comparable degrees of 30 nm fiber formation. Moreover, Mg^{2+} affects the internal mobility in polynucleosome fragments shorter than 6–7 nucleosomes, which are too short to be compacted by Na^+. On the basis of these observations we suggest that the chromatin is packed in a more "tight" conformation by Mg^{2+}. The more rigid conformation is possibly caused by Mg^{2+}-promoted interactions between consecutive linker DNA segments in a crosswise 30 nm chromatin fiber.

Macroscopic aggregates are formed at Mg^{2+} concentrations above 0.2–0.3 m*M*. However, the aggregation is uncorrelated with the more rapid intramolecular compaction.

Finally, we note a correlation between the ethidium binding constant and the internal chromatin flexibility. We point out that the correlation may arise from the lower torsional and "unwinding" flexibility of linker DNA segments in compacted chromatin fibers.

References

Allison SA, Schurr JM (1979) Torsion dynamics and depolarization of linear macromolecules. I. Theory and application to DNA. Chem Phys 41:35–39

Angerer LM, Moudrianakis EN (1972) Interaction of ethidium bromide with whole and selectively deproteinized deoxynucleoprotein from calf thymus. J Mol Biol 63:505–521

Ashikawa I, Kinosita K Jr, Ikegami A, Nishimura Y, Tsuboi M, Watanabe K, Iso K, Nakano T (1983) Internal motion of deoxyribonucleic acid in chromatin. Nanosecond fluorescence studies. Biochemistry 22:6018–6026

Ashikawa I, Kinosita K Jr, Ikegami A, Nishimura Y, Tsuboi M (1985) Increased stability of the higher order structure of chicken erythrocyte chromatin: nanosecond anisotropy studies of intercalated ethidium. Biochemistry 24:1291–1297

Barkley MD, Zimm BH (1979) Theory of twisting and bending of chain macromolecules; analysis of the fluorescence depolarization of DNA. J Chem Phys 70:2991–3007

Bordas J, Perez-Grau L, Koch MHJ, Vega MC, Nave C (1986) The superstructure of chromatin and its condensation mechanism. I. Synchroton radiation X-ray scattering results. Eur Biophys J 13:157–173

Bordas J, Perez-Grau L, Koch MHJ, Vega MC, Nave C (1986) The superstructure of chromatin and its condensation mechanism. II. Theoretical analysis of the X-ray scattering patterns and model calculations. Eur Biophys J 13:175–185

Butler PJG (1983) The folding of chromatin. CRC Crit Rev Biochem 15:57–91

Butler PJG, Thomas JO (1980) Changes in chromatin folding. J Mol Biol 140:505–529

Cantor CR, Schimmel PR (1980) In: Biophysical chemistry, Part II. Freeman, San Francisco

Chauvin F, Roux B, Marion C (1985) Higher order structure of chromatin: influence of ionic strength and proteolytic digestion on the birefringence properties of polynucleosomal fibers. J Biomol Struct Dyn 2(4):805–819

Felsenfeld G, McGhee JD (1986) Structure of the 30 nm chromatin fiber. Cell 44:375–377

Finch JT, Klug A (1976) Solenoidal model for the superstructure of chromatin. Proc Natl Acad Sci USA 73:1897–1901

Fulmer AW, Bloomfield VA (1982) Higher order folding of two different classes of chromatin isolated from chicken erythrocyte nuclei: a light scattering study. Biochemistry 21:985–992

Genest D, Sabeur G, Wahl P, Auchet J-C (1981) Fluorescence anisotropy decy of ethidium bound to chromatin. Biophys Chem 13:77–87

Gerchman SE, Ramakrishnan V (1987) Chromatin higher-order structure studied by neutron scattering and scanning transmission electron microscopy. Proc Natl Acad Sci USA 84:7802–7806

Greulich KO, Wachtel E, Ausio J, Seger D, Eisenberg H (1987) Transition of chromatin from the "10 nm" lower order structure to the "30 nm" higher order structure as followed by small-angle X-ray scattering. J Mol Biol 193:709–721

Harrington RE (1985) Optical model studies of the salt-induced 10–30 nm fiber transition in chromatin. Biochemistry 24: 2011–2021

Härd T (1987) Out-of-plane mobility in the ethidium/DNA complex. Biopolymers 26:613–618

Härd T, Kearns DR (1986 a) Anisotropic motions in intercalative DNA/Dye complexes. J Phys Chem 90:3437–3444

Härd T, Kearns DR (1986 b) Association of short DNA fragments: fluorescence polarization study. Biopolymers 25: 1519–1529

Heyn MP (1979) Determination of lipid order parameters and rotational correlation times from fluorescence depolarization experiments. FEBS Lett 108(2):359–364

Kinosita K Jr, Kawato S, Ikegami A (1977) A theory of fluorescence polarization decay in membranes. Biophys J 20:289–305

Koch MHJ, Vega MC, Sayers Z, Michon AM (1987) The superstructure of chromatin and its condensation mechanism. III. Effect of monovalent and divalent cations on X-ray solution scattering. Eur Biophys J 14:307–319

Kubista M, Härd T, Nielsen PE, Nordén B (1985) Structural transitions of chromatin at low salt concentrations. A flow linear dichroism study. Biochemistry 24:6336–6342

Kubista M, Nielsen PE, Hagmar P, Nordén B (1988) Flow-linear dichroism supports an accordion model for the salt-induced condensation of chromatin. Biochem Pharmacol 37:1813–1814

Lerner MR, Steitz IA (1979) Antibodies to small nuclear RNAs complexed with proteins are produced by patients with systemic lupus erythematosus. Proc Natl Acad Sci USA 76:5495–5499

Magde D, Zappala M, Knox WH, Nordlund TM (1983) Picosecond fluorescence anisotropy decay in the ethidium/DNA complex. J Phys Chem 87:3286–3288

Makarov V, Dimitrov SI, Petrov PT (1983) Salt-induced conformational transitions in chromatin: A flow linear dichroism study. Eur J Biochem 133:491–497

Makarov V, Dimitrov S, Smirnov V, Pashev I (1985) A triple helix model for the structure of chromatin fiber. FEBS Lett 181:357–361

Makarov V, Smirnov I, Dimitrov SI (1987) Higher order folding of chromatin is induced in different ways by monovalent and by divalent cations. FEBS Lett 212:265–266

Marion C (1984) The structural organization of oligonucleosomes. J Biomol Struct Dyn 2(2):303–317

Marion C, Bezot P, Hesse-Bezot C, Roux B, Bernengo J-C (1981) Conformation of chromatin oligomers. A new argument for a change with the hexanucleosome. Eur J Biochem 120:169–178

Marquet R, Colson P, Houssier C (1986) The condensation of chromatin and histone H1-depleted chromatin by spermine. J Biomol Struct Dyn 4:205–217

McGhee JD, Rau DC, Charney E, Felsenfeld G (1980) Orientation of the nucleosome within the higher structure of chromatin. Cell 22:87–96

McGhee JD, Nickol JM, Felsenfeld G, Rau DC (1983) Higher order structure of chromatin: orientation of nucleosomes within the 30 nm chromatin solenoid is independent of species and spacer length. Cell 33:831–841

Nielsen PE (1985) Development and application of photochemical probes for studying protein-DNA interactions in eukaryotic chromatin. K Dan Vidensk Selsk Biol Skr 24:91–121

Paoletti J, Magee BB, Magee PT (1977) The structure of chromatin: interaction of ethidium bromide with native and denaturated chromatin. Biochemistry 16:351–357

Richmond TJ, Finch JT, Rushton B, Rhodes D, Klug A (1984) Structure of the nucleosome core particle at 7 Å resolution. Nature 311:532–537

Sen D, Crothers DM (1986) Condensation of chromatin: role of multivalent cations. Biochemistry 25:1495–1503

Shibata JH, Fujimoto BS, Schurr JM (1985) Rotational dynamics of DNA from 10^{-10} to 10^{-5} seconds: comparison of theory with optical experiments. Biopolymers 24:1909–1930

Suau P, Bradbury EM, Baldwin JP (1979) Higher-order structure of chromatin in solution. Eur J Biochem 97:593–602

Subirana JA, Munoz-Guerra S, Radermacher M, Frank J (1983) Three-dimensional reconstruction of chromatin fibers. J Biomol Struct Dyn 1:705–714

Szabo A (1984) Theory of fluorescence depolarization in macromolecules and membranes. J Chem Phys 81:150–167

Thoma F, Koller Th, Klug A (1979) Involvement of histone H1 in the organization of the nucleosome and of the salt-dependent superstructures of chromatin. J Cell Biol 83:403–427

Tjerneld F, Nordén B, Wallin H (1962) Chromatin structure studied by linear dichroism at different salt concentrations. Biopolymers 21:343–358

Waring MJ (1965) Complex formation between ethidium bromide and nucleic acids. J Mol Biol 13:269–282

Watanabe K, Kuojiro I (1984) Magnesium binding and conformational change of DNA in chromatin. Biochemistry 23:1376–1383

Widom J, Klug A (1985) Structure of the 300 Å chromatin filament: X-ray diffraction from oriented samples. Cell 43: 207–213

Widom J (1986) Physicochemical studies of the folding of the nucleosome filament into the 300 Å filament. J Mol Biol 190:411–424

Williams SP, Athey BD, Muglia LJ, Schappe RS, Gough AH, Langmore JP (1986) Chromatin fibers are left-handed double helices with diameter and mass per unit that depend on linker length. Biophys J 49:233–248

Woodcock CLF, Frado L-LY, Rattner JB (1984) The higher-order structure of chromatin: Evidence for a helical ribbon arrangement. J Cell Biol 99:42–52

Worcel A, Strogatz S, Riley D (1981) Structure of chromatin and the linking number of DNA. Proc Natl Acad Sci USA 78:1461–1465